PHYSICAL REVIEW C **76**, 011304(R) (2007)

Level structure of ^{92}Rh: Implications for the two-proton decay of ^{94}Ag^{m}

O. L. Pechenaya,[1] C. J. Chiara,[2] D. G. Sarantites,[2] W. Reviol,[2] R. J. Charity,[2] M. P. Carpenter,[3] R. V. F. Janssens,[3] T. Lauritsen,[3] C. J. Lister,[3] D. Seweryniak,[3] S. Zhu,[3] L.-L. Andersson,[4] E. K. Johansson,[4] and D. Rudolph[4]

[1]*Department of Physics, Washington University, St. Louis, Missouri 63130, USA*

[2]*Department of Chemistry, Washington University, St. Louis, Missouri 63130, USA*

[3]*Physics Division, Argonne National Laboratory, Argonne, Illinois 60439, USA*

[4]*Department of Physics, Lund University, S-22100 Lund, Sweden*

(Received 11 May 2007; published 19 July 2007)

The 21^{+} isomer in ^{94}Ag has recently been reported to have a two-proton decay branch to ^{92}Rh. We have populated ^{92}Rh through the ^{40}Ca(^{58}Ni,αpn) reaction at 240 MeV, and have performed detailed spectroscopic measurements of the levels, finding new states and measuring angular distributions of γ rays. We find no evidence for the states reported to be populated by the two-proton decay of ^{94}Ag^{m}. The calculated Q-value for the two-proton decay implies that this process directly feeds low-lying yrast, or near-yrast, states in ^{92}Rh, which is very difficult to reconcile with our observations. Several scenarios for the population of ^{92}Rh are discussed, none of which appears to be satisfactory.

DOI: 10.1103/PhysRevC.76.011304 PACS number(s): 23.20.Lv, 23.50.+z, 23.20.En, 27.60.+j

The two-proton decay mode provides information relevant to the wave functions of states of very proton-rich nuclei. Of particular interest are two-proton decays characterized by the nonsequential emission of two protons, bypassing any unbound state in the one-proton daughter, which affords insight into the correlations between nucleons. In 1960, Goldansky predicted that correlated two-proton decay might be observed in medium-mass ($16 \leqslant A \leqslant 67$), even-$Z$ nuclei [1]. Goldansky and Peker later calculated that this decay mode would also occur in many-particle isomeric states in heavier nuclei, specifically ^{82}Mo^{m}, ^{96}Cd^{m}, ^{106}Te^{m}, and ^{108}Te^{m} [2]. Correlated two-proton emission remains unconfirmed in medium-mass and heavier nuclei, although several experimental attempts have been made to observe it (e.g., in ^{45}Fe, ^{48}Ni, and ^{54}Zn [3–5]).

A recent publication [6] presents evidence for correlated two-proton decay of the $I^{\pi} = 21^{+}$, 6.7-MeV, $t_{1/2} = 0.39(4)$ s isomeric state in ^{94}Ag. This state is unique in several ways: it has the highest known spin for a β-decaying state [7], and, if confirmed, it will be the only state known so far to exhibit competing β-, one-proton, and two-proton decay modes. The two branches of one-proton decay of ^{94}Ag^{m} were reported by the same authors earlier [8]. Reference [6] reports the two protons as having a sum energy of 1.9(1) MeV, an angular momentum $6 \leqslant L \leqslant 10$, and representing a decay branch of 0.5(3)%. The authors of Ref. [6] propose that ^{94}Ag^{m} must be highly deformed, with a major-to-minor axis ratio greater than 2 (cigar-shaped) to explain the large partial half-life (80^{+110}_{-30} s).

A calculation of the energy available (Q-value) for the two protons places a severe constraint on the range of states in ^{92}Rh available to be populated by two-proton decay. The essential equation for the Q-value is $\Delta(^{94}\mathrm{Ag}) + E^{*}(^{94}\mathrm{Ag}) = \Delta(^{92}\mathrm{Rh}) + E^{*}(^{92}\mathrm{Rh}) + E_{2p} + 2\Delta p$. Table I explains the symbols and provides the numerical values. We reduced the uncertainty in our calculation by recognizing that the left side of the equation above is also valid for one-proton decay, since the energy of the excited state of ^{94}Ag was derived from the observation of the two one-proton decay branches to ^{93}Pd in Ref. [8]. Hence, we can eliminate ^{94}Ag-related terms and rewrite the equation as $\Delta(^{93}\mathrm{Pd}) + E^{*}(^{93}\mathrm{Pd}) + \Delta p + E_{p} = \Delta(^{92}\mathrm{Rh}) + E^{*}(^{92}\mathrm{Rh}) + 2\Delta p + E_{2p}$. Note that the error in the measured energies of the protons is less than the error in the mass excess of ^{94}Ag, and that using the present approach we reproduced the Q-value cited in Ref. [8]. Systematic errors in the extrapolated mass excess values of ^{93}Pd and ^{92}Rh are likely to both be in the same direction. As they appear on opposite sides of the above relation, they will partially cancel, reducing the overall uncertainty in the deduced value of $E^{*}(^{92}\mathrm{Rh})$. The calculation gives the most probable excitation energy in ^{92}Rh which two-proton decay may populate as 0.24(57) MeV. Thus, it is desirable to improve the ^{92}Rh level scheme, which was previously obtained from in-beam work [11]. Special attention needs to be drawn to the unplaced 307-keV transition [11] and the newly reported 565- and 833-keV transitions [6] with the goal of examining the possible paths for the two-proton decay of ^{94}Ag^{m}.

This Rapid Communication presents results of an experiment exploring the proton-rich $A \sim 90$ nuclei. These data allowed us to improve the previous ^{92}Rh level scheme, find new transitions, investigate the existence of the transitions reported in Ref. [6], and, in the process, investigate the constraints on the probability of two-proton decay of ^{94}Ag^{m} based on energy conservation and the difference in angular momentum between the parent and daughter nuclei.

States in ^{92}Rh were populated via the ^{40}Ca(^{58}Ni,αpn) fusion-evaporation reaction. The ATLAS accelerator at Argonne National Laboratory delivered the 240-MeV ^{58}Ni beam. The target consisted of 0.40 mg/cm^2 of ^{40}Ca, sandwiched between two layers of 0.15 mg/cm^2 of gold to reduce possible oxidization. The Gammasphere Ge-detector array [12] was used for γ-ray detection. The five most forward rings of Gammasphere were replaced with the Neutron Shell [13] of liquid-scintillator neutron detectors. Thus, a total of 76 Ge detectors and 30 liquid scintillators were present during the experiment. A hardware veto of the γ-ray flash detected by

TABLE I. Values (all in MeV) used in the Q-value calculations discussed in the text. Δ is the mass excess of the given nucleus [9,10]. E^* is the excitation energy of ^{94}Ag^m, the state in ^{93}Pd populated by single-proton decay, or the calculated most probable energy value for ^{92}Rh; E is the kinetic energy of the protons. Both branches of one-proton decay of ^{94}Ag^m are listed. The calculated E^* of ^{92}Rh is the average of the two possible values.

	^{94}Ag	^{93}Pd	^{92}Rh	p	$2p$
Δ	−53.30(50)	−59.70(40)	−63.36(40)	7.29(0)[a]	–
E^*	6.7(3)[b]	4.994[b]	0.24(57)	–	–
	–	4.751[b]	–	–	–
E	–	–	–	0.79(3)[b]	1.9(1)[c]
	–	–	–	1.01(3)[b]	–

[a]Error negligible ($<10^{-3}$).
[b]Reference [8].
[c]Reference [6].

the liquid-scintillator detectors helped to enhance the neutron events in the data set. The Microball array of 95 CsI(Tl) detectors was used to detect light charged particles [14]. Data from the Argonne Fragment Mass Analyzer (FMA) [15] were also included in the data stream for part of the experiment, but the statistics for mass $A = 92$ events were too low for inclusion in the present analysis.

The trigger condition required the detection of at least five coincident γ rays, or a liquid scintillator event plus two coincident γ rays. Signals from the Microball and the FMA were not required in the trigger, but were recorded if present. A total of 2.5×10^9 events were recorded. Of these, 3×10^7 events were assigned to the αpn channel, sorted such that events containing exactly one detected α particle, one proton, and one neutron were selected. In the offline analysis, the Microball efficiencies were determined to be about 60% for α particles and 70% for protons. The Neutron Shell efficiency for single neutron detection was measured to be 30% as discussed in Ref. [13]. Prompt γ rays were sorted into two-dimensional histograms of γ-ray energies (E_γ-E_γ matrices). The software package RADWARE [16] was used to establish mutual coincidences and measure relative intensities of γ rays.

Figure 1(a) shows a typical spectrum from the data set. A search for γ rays coincident with known ^{92}Rh γ rays [11] revealed two new transitions with energies of 1114 and 1939 keV. The evidence for the new transitions is supported by mutual coincidences between these two lines and other transitions in the negative-parity sequence of ^{92}Rh. Figure 2 presents the level scheme of ^{92}Rh deduced in this work. Most aspects of the previously reported level scheme [11] have been confirmed. The previously tentative 307-keV γ ray was assigned as the 306-keV $20^{(-)} \rightarrow 19^{(-)}$ transition. The 575-keV transition, also tentative in Ref. [11], was not observed [see Fig. 1(a) and 1(b)]. Based on intensity considerations, the 632-keV γ ray was placed higher in spin as the $19^{(-)} \rightarrow 18^{(-)}$ transition and the order of the 939- and 1034-keV transitions has been reversed. The lowest observed state of ^{92}Rh was previously designated as 6^+ on the basis of shell model calculations [11]. The latest experimental information available for the ground state decay gives a spin value of $\geqslant 5$, with no parity assignment [17]. Since this is not sufficient evidence to specify the ground state quantum number, all spin assignments proposed here are relative to an assumed 6^+ assignment for the lowest observed state.

The angular distributions of γ rays measured with respect to the spin axes of the evaporation residues were used to determine their multipolarities. The momenta of evaporated particles were measured with the Microball and the Neutron Shell. The recoil kicks imparted to each residue by the evaporation particles were consequently determined, yielding the direction of motion for the residues. The directions of the residue and the beam define a reaction plane for each event. The spin axis is then assumed to be perpendicular to this plane. The data were sorted into $E_\gamma(\theta) - E_\gamma(\text{any})$ matrices,

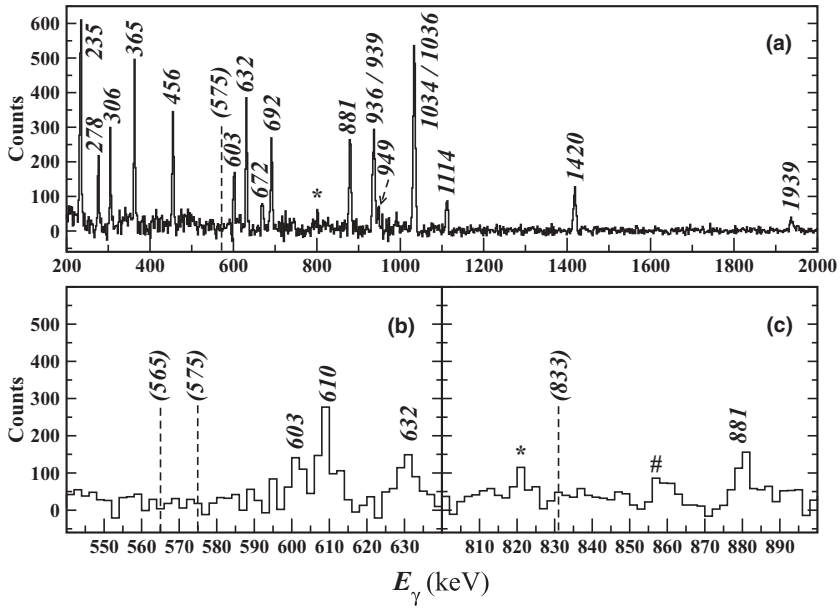

FIG. 1. (a) Sample spectrum from an E_γ-E_γ coincidence matrix, gated by 939 keV (the gate overlaps with 936 keV). All transitions identified by their energies in keV are from ^{92}Rh. The spectra have a dispersion of 2 keV per channel. The spectra in panels (b) and (c) are produced by gating on 365 keV, and show the absence of the 565- and 833-keV transitions claimed by Ref. [6]. Panels (a) and (b) also show the absence of the tentative 575-keV transition from Ref. [11]. The asterisk and the pound sign indicate contaminant transitions from ^{91}Ru and ^{91}Tc, respectively.

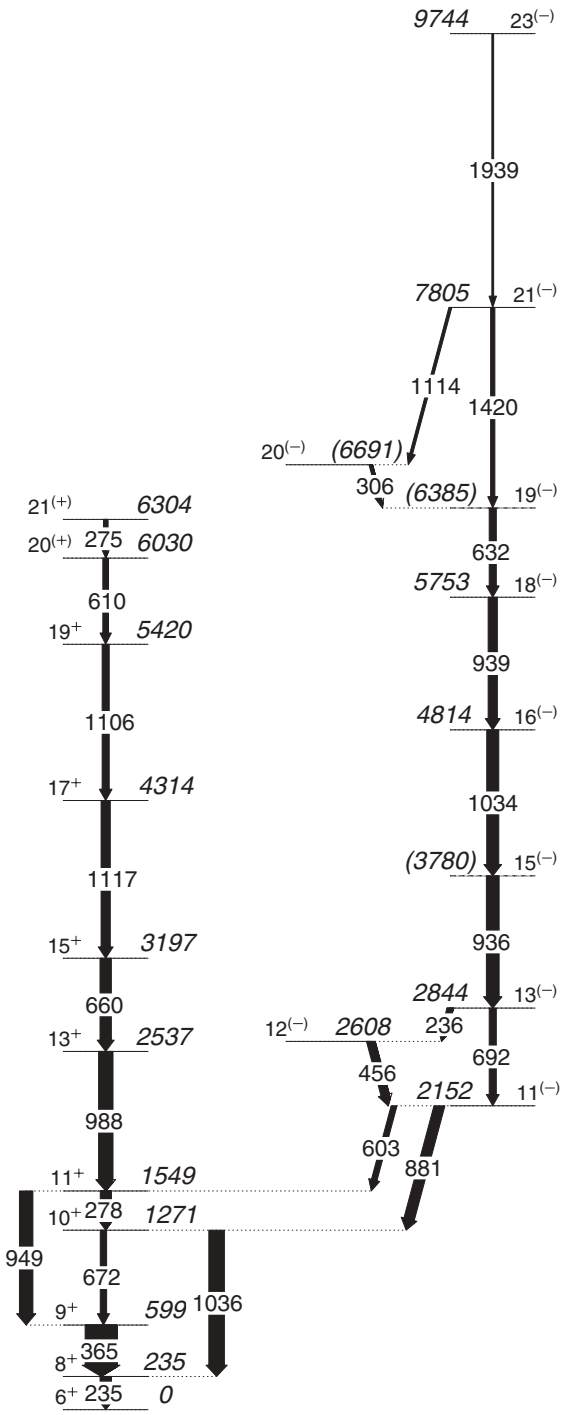

FIG. 2. Level scheme of ^{92}Rh as deduced in this work. The widths of the arrows are proportional to the relative intensities of the γ rays (Table II gives the numerical values). The intensity of the 235-keV transition is reported as observed in a matrix of prompt coincident γ rays, with the remaining intensity populating the 6^+ state unobserved due to isomerism. The energies of levels relative to the lowest state and the transition energies are given in keV. The 6^+ spin-parity assignment for the lowest state has been adopted from previous work [11]. The negative parities are uncertain due to factors discussed in the text. The order of the 936- and 1034-keV transitions is uncertain due to similar intensities. Same is true for the 632- and 1420-keV (plus accompanying) transitions.

where θ represents the angle between the emitted γ ray and the spin axis (binned into 15° increments), and "any" indicates that there is no angle requirement. The latter axis is used for gating purposes. This method provides larger anisotropies of the angular distribution function $W(\theta)$, expressed as $W(90°)/W(0°)$, than those obtained by measuring angular distributions relative to the beam axis, where the inverse anisotropies $W(0°)/W(90°)$ are used. This method will be elucidated in a forthcoming publication [18].

A computer code [19] was used to calculate angular distributions for given spin sequences. The input parameters for each sequence were the initial (I_i) and final spin (I_f) of each transition; the alignment parameter (σ/I) where σ represents the standard deviation of a Gaussian distribution for the population of spin substates; and the quadrupole/dipole ($E2/M1$) mixing ratio δ. A least-squares fitting routine gave the best combination of parameters based on measured angular distributions for each γ ray, which then allowed the assignment of spins as given in Table II. Figure 3 provides samples of the angular distributions and the calculated curves for two

TABLE II. Properties of γ rays observed in this work. The intensities are given relative to the total intensity populating the 8^+ state. The initial and final spins I are given together with the parities π. The standard deviation of the Gaussian distribution of the spin substates, with respect to spin (σ/I), and the $E2/M1$ mixing ratios (δ) were calculated using a code described in the text. The anisotropies (last column) were derived from the calculated curves.

E_γ(keV)	Int.	I_i^π	I_f^π	σ/I	$\delta(E2/M1)$	$\frac{W(90°)}{W(0°)}$
236	18.0(7)	$13^{(-)}$	$12^{(-)}$	0.28(5)	−0.07(3)	0.60(5)
275	12.0(6)	$21^{(+)}$[a]	$20^{(+)}$	0.23(4)	−0.04(6)	0.60(8)
278	30(3)	11^+[b]	10^+	0.23(4)	0.01(5)	0.68(8)
306	10.0(8)	$20^{(-)}$	$19^{(-)}$	0.29(5)	0.11(5)	0.92(8)
365	56(7)	9^+	8^+	0.23(4)	−0.05(3)	0.57(5)
456	24.0(23)	$12^{(-)}$	$11^{(-)}$	0.28(5)	−0.05(5)	0.63(7)
603	16.0(14)	$11^{(-)}$	11^+	–	–	–
610	16.0(12)	$20^{(+)}$	19^+	0.21(6)	−0.05(3)	0.57(4)
632	20.0(13)	$19^{(-)}$	$18^{(-)}$	0.27(7)	0.25(4)	1.33(13)
660	32.0(21)	15^+	13^+	0.26(7)	–	1.86(39)
672	18.0(9)	10^+	9^+	0.23(4)	−0.20(6)	0.39(6)
692	20.0(13)	$13^{(-)}$	$11^{(-)}$	0.30(6)	–	1.70(25)
881	30(3)	$11^{(-)}$	10^+	0.28(5)	−0.02(4)1[a]	0.68(7)
936	36(3)	$15^{(-)}$	$13^{(-)}$	0.27(5)	–	1.83(24)
939	26(4)	$18^{(-)}$	$16^{(-)}$	0.26(5)	–	1.84(26)
949	38.0(21)	11^+[b]	9^+	0.23(4)	–	2.12(28)
988	40.0(23)	13^+	11^+	0.20(4)	–	2.34(37)
1034	34(3)	$16^{(-)}$	$15^{(-)}$	0.27(7)	0.27(5)	1.43(20)
1036	44(7)	10^+	8^+	0.23(5)	–	2.11(38)
1106	20.0(6)	19^+	17^+	0.23(5)	–	2.06(57)
1114	8.0(2)	$21^{(-)}$	$20^{(-)}$	0.26(5)	−0.14(9)	0.50(10)
1117	26.0(21)	17^+	15^+	0.19(6)	–	2.37(70)
1420	12.0(9)	$21^{(-)}$	$19^{(-)}$	0.29(5)	–	1.70(21)
1939	5.0(6)	$23^{(-)}$	$21^{(-)}$	0.25(7)	–	1.90(42)

[a]The deduced mixing ratios for the 275-, 610-, and 881-keV γ rays are consistent with stretched $E1$ assignments (see text for details).
[b]The parity assignment is based on the 949-keV $E2$ transition.

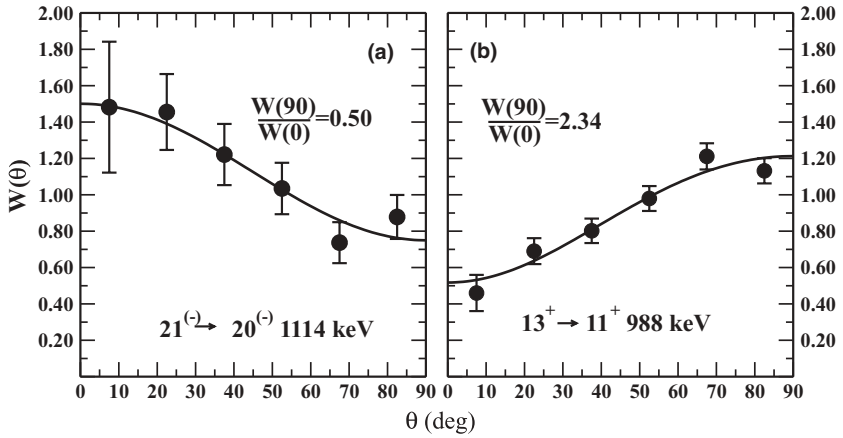

FIG. 3. Measured (data points) and calculated (lines) angular distributions relative to the residue spin axis for (a) the 1114-keV and (b) the 988-keV γ rays.

^{92}Rh γ rays. The $8^+ \rightarrow 6^+$, 235-keV transition could not be analyzed in the present work because the 8^+ state is long-lived (a Weisskopf estimate gives $t_{1/2} = 34$ ns). No multipolarity assignment was obtained for the 603-keV transition due to poor statistics. The anisotropy of the 881-keV γ ray is characteristic of a stretched dipole transition; however, since the value of δ is consistent with zero (see Table II), it is not possible to distinguish between $E1$ and $M1$ multipolarities. Thus, we adopt the parity assignments of Ref. [11] for this transition and the sequence above it. The parity assignments of Ref. [11] were based on systematics of neighboring nuclei and shell-model calculations. The mixing ratios for the 610- and 275-keV transitions which top the positive-parity sequence are also consistent with zero, therefore we tentatively assign the $20^{(+)}$ and $21^{(+)}$ state based on the same considerations. While the same may be said about the 278-keV transition, the spin and parity assignment of its initial state is established by the strong $E2$ character of the 949-keV transition.

The γ rays at 565 and 833 keV proposed in Ref. [6] are not observed in this work. Analysis of spectra gated by known transitions in ^{92}Rh provides an upper limit on their intensity of less than 4% of the total observed intensity populating the first excited state (8^+). Two sections of a sample spectrum obtained by gating on the 365-keV line are given in Fig. 1(b) and 1(c). Specifically, our analysis rules out the presence of prominent γ rays with energies of 565 and 833 keV in prompt coincidence with each other and/or with any of the known γ rays in ^{92}Rh, most notably below the 11^+ state.

The possible existence of these transitions in ^{92}Rh, however, is not completely ruled out. These states might not be populated in the fusion-evaporation process, yet they could have been observed in decay work such as the work described in Ref. [6]. The spectrum in Fig. 1(d) of Ref. [6] shows both previously known and these two unknown transitions with similar intensity in coincidence with two protons. There may, then, be a second branch of two-proton decay which populates states producing the 565- and 833-keV transitions. Hence, let us consider possible scenarios in which the 565- and 833-keV γ rays may fit into the level structure of ^{92}Rh such that the two protons are in coincidence with them.

Three examples of such scenarios are shown in Fig. 4, in which the two transitions reported by Ref. [6] are placed so that the two protons carry L units of angular momentum, and populate a state directly above at (I) 2947 keV ($L = 6$); (II) 1633 keV ($L = 9$); and (III) 1398 keV ($L = 11$). Here it is assumed, as implied in Ref. [6], that the 565- and 833-keV transitions take up to 4 units of angular momentum, i.e., they are of stretched quadrupole character, and in coincidence with each other. The two γ rays in these scenarios would, therefore, populate the 11^+, 8^+, or 6^+ state in ^{92}Rh, respectively.

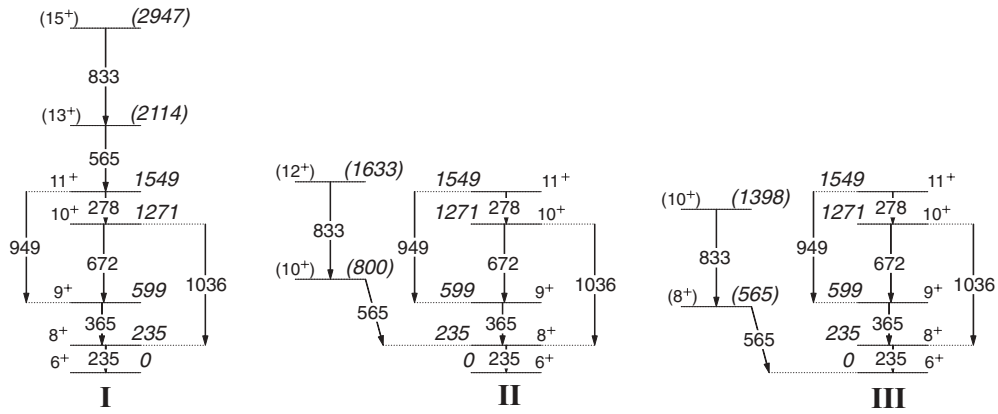

FIG. 4. Three scenarios for the ^{94}Ag^m 2p-decay considered in the text, in which the two protons populate states directly above the 565- and 833-keV transitions of Ref. [6]. These transitions are assumed to be quadrupoles and in coincidence with each other.

Scenario I is presented in Ref. [6] as it is, of the scenarios considered, the only one that is consistent with an angular momentum $L = 6$. This scenario is ruled out by the Q-value calculation to a confidence limit of 99.9997%. Also, the states populated would be yrast (possessing the lowest energy for a given spin), and thus would most likely be populated in our fusion-evaporation reaction.

The same can be said about scenario II, in which the two protons populate an unplaced yrast 12^+ state. This scenario is ruled out to a 98% confidence limit. More notably, both scenarios I and II are ruled out by our in-beam study, because the 565- and 833-keV γ rays were not observed in our data.

In the third scenario considered, the two protons may populate a 1398-keV 10^+ state, which makes this a nonyrast case. This case is ruled out to a 96% confidence limit. In addition, the third scenario requires removal of 11 units of angular momentum. This would, according to the calculations in Ref. [6], imply an even larger deformation ($>4:1$ axis ratio) for ^{94}Ag^m. Finally, if the 565- and 833-keV transitions are not in coincidence with each other and/or if either has $\Delta I < 2$, the angular momentum carried by the two protons must be greater still, thus strengthening the argument for rejection of all scenarios.

Disregarding the possible existence of the 565- and 833-keV γ rays, let us consider the two protons populating the 8^+ or the 9^+ state in ^{92}Rh directly, as the energies of each are within one standard deviation of the Q-value calculated above. The two protons would then carry 13 or 12 units of angular momentum, respectively, not 6 to 10 as suggested by Ref. [6]. If either of these is the case, the state in the parent nucleus must be, again, even more deformed than calculated in Ref. [6] for the two protons to have the reported partial half-life of 80^{+110}_{-30} s, provided that the treatment of the ^{94}Ag^m parent state as a deformed state is valid. Population of any state above the 9^+ is ruled out to at least a 93% confidence limit.

It must be noted that, although ^{94}Ag^m was assumed to be highly deformed in the calculations of Ref. [6], a separate calculation [20] using the cranked Nilsson-Strutinsky approach [21] indicates that ^{94}Ag^m is almost spherical. This calculation predicts an axis ratio of $1.06:1$, and that, to have an axis ratio of $2:1$, the energy of the 21^+ state of ^{94}Ag would have to be 10 MeV higher than was observed in Ref. [6].

To summarize, in this work we have presented an updated level scheme for ^{92}Rh. Measured angular distributions were used to establish the multipolarities of most observed transitions. The new information, along with Q-value and energy considerations, was used to evaluate scenarios for two-proton decay from ^{94}Ag^m. While this decay mode cannot be ruled out, the constraints placed by this work point to a spin difference $\Delta I > 10$ between the initial and final states in the parent and daughter nuclei, respectively. This is in conflict with Ref. [6], as it reduces the likelihood for that mode considerably.

The authors would like to acknowledge valuable discussions with A. Stuchbery and I. Ragnarsson. This work was supported in part by the U.S. Department of Energy, Office of Nuclear Physics, under Grant No. DE-FG02-88ER-40406 and Contract No. DE-AC02-05CH11357, and by the Swedish Research Council.

[1] V. I. Goldansky, Nucl. Phys. **19**, 482 (1960).
[2] V. I. Gol'danskii and L. K. Peker, JETP Lett. **13**, 412 (1971).
[3] J. Giovinazzo *et al.*, Phys. Rev. Lett. **89**, 102501 (2002).
[4] C. Dossat *et al.*, Phys. Rev. C **72**, 054315 (2005).
[5] B. Blank *et al.*, Phys. Rev. Lett. **94**, 232501 (2005).
[6] I. Mukha *et al.*, Nature (London) **439**, 298 (2006).
[7] C. Plettner *et al.*, Nucl. Phys. **A733**, 20 (2004).
[8] I. Mukha *et al.*, Phys. Rev. Lett. **95**, 022501 (2005).
[9] A. H. Wapstra, G. Audi, and C. Thibault, Nucl. Phys. **A729**, 129 (2003).
[10] G. Audi, A. H. Wapstra, and C. Thibault, Nucl. Phys. **A729**, 337 (2003).
[11] D. Kast *et al.*, Z. Phys. A **356**, 363 (1997).
[12] I. Y. Lee, Nucl. Phys. **A520**, 641c (1990).
[13] D. G. Sarantites *et al.*, Nucl. Instrum. Methods Phys. Res. A **530**, 473 (2004).
[14] D. G. Sarantites, P.-F. Hua, M. Devlin, L. G. Sobotka, J. Elson, J. T. Hood, D. R. LaFosse, J. E. Sarantites, and M. R. Maier, Nucl. Instrum. Methods Phys. Res. A **381**, 418 (1996).
[15] C. N. Davids, B. B. Back, K. Bindra, D. J. Henderson, W. Kutschera, T. Lauritsen, Y. Nagame, P. Sugathan, A. V. Ramayya, and W. B. Walters, Nucl. Instrum. Methods Phys. Res. B **70**, 358 (1992).
[16] D. C. Radford, Nucl. Instrum. Methods Phys. Res. A **361**, 297 (1995).
[17] S.-W. Xu *et al.*, Phys. Rev. C **71**, 054318 (2005).
[18] C. J. Chiara *et al.*, Nucl. Instrum. Methods Phys. Res. (to be submitted).
[19] A. Stuchbery (private communication).
[20] I. Ragnarsson and B. G. Carlsson, http://www.phy.ornl.gov/ns06/NS06-Book-Abstracts.pdf (2006); (private communication).
[21] A. V. Afanasjev, D. B. Fossan, G. J. Lane, and I. Ragnarsson, Phys. Rep. **322**, 1 (1999).